Geochemistry Geophysics Geosystems G3
AN ELECTRONIC JOURNAL OF THE EARTH SCIENCES
Published by AGU and the Geochemical Society

Technical Brief
Volume 4, Number 1
XX Month 2003
XXXX, doi:10.1029/2003GC000509
ISSN: 1525-2027

A method for Doppler acoustic measurement of black smoker flow fields

Darrell R. Jackson and Christopher D. Jones
Applied Physics Laboratory, University of Washington, Seattle, Washington 98105, USA (drj@apl.washington.edu)

Peter A. Rona and Karen G. Bemis
Institute of Marine and Coastal Sciences and Department of Geological Sciences, Rutgers University, New Brunswick, New Jersey, USA

[1] A method is developed for using multibeam sonar to map the flow velocity field of black smoker plumes. The method is used to obtain two-dimensional (2-D) cross-sectional maps of vertical velocity, but is capable of mapping velocity in three dimensions. This is in contrast to conventional current meters, which measure only at several points and acoustic Doppler current profilers, whose diverging beams cannot readily map the interior of a plume. Geometric corrections are used to estimate the vertical component of velocity, compensating for ambient current. The method is demonstrated using data from the main plume at the Grotto vent complex in the Main Endeavour Field, Juan de Fuca Ridge, and the errors due to noise, signal fluctuations, and fluctuations in plume structure are estimated.

Components: 6,732 words, 5 figures.

Keywords: Hydrothermal.

Index Terms: 3015 Marine Geology and Geophysics: Heat flow (benthic) and hydrothermal processes; 4259 Oceanography: General: Ocean acoustics; 3094 Marine Geology and Geophysics: Instruments and techniques.

Received 13 January 2003; **Revised** 5 September 2003; **Accepted** 26 September 2003; **Published** XX Month 2003.

Jackson, D. R., C. D. Jones, P. A. Rona, and K. G. Bemis, A method for Doppler acoustic measurement of black smoker flow fields, *Geochem. Geophys. Geosyst.*, *4*(1), XXXX, doi:10.1029/2003GC000509, 2003.

1. Introduction

[2] Plumes that discharge from high-temperature black smoker-type vents at ocean ridges are being intensively studied as major agents of dispersal of heat, chemicals, and biological material. The buoyant plume entrains and mixes with ambient seawater as it rises tens to hundreds of meters to a level of neutral buoyancy. Standard methods of study involve making asynchronous individual profiles of temperature, salinity and light attenuation or scattering versus depth (CTD-transmissometer-nephelometer profiles [*Lupton*, 1995; *Baker et al.*, 1995]). Acoustic Doppler current profilers (ADCPs) have been used to study flow velocity [*Palmer and Rona*, 1990; *Mitsuzawa*, 2003], but cannot readily map out the velocity field in three-dimensional (3-D) or in 2-D cross sections. First, ADCPs do not provide either 3-D images or 2-D cross sections, so there is a problem in locating the data with respect to the plume boundaries. Second, because their sonar beams diverge in space, ADCPs cannot readily provide meter-scale resolution at the decimeter ranges required for plume observations. We report here on development of a Doppler method to measure the vertical velocity

field of hydrothermal plumes. This velocity measurement, in concert with sonar measurements of plume structure (via mapping of the acoustic backscattering strength) such as those we have reported previously [*Rona et al.*, 1991; *Bemis et al.*, 2000; *Rona et al.*, 2001], is important to the understanding of plume behavior. The goal of this paper is to demonstrate the method using a limited set of data. It is expected that, with larger data sets, the method will be useful for tests of plume models.

[3] The data used to illustrate the method were obtained as part of the Vent Imaging Pacific 2000 (VIP 2000) cruise during which several types of sonar observations were made within the Main Endeavour Field on the Juan de Fuca Ridge. These measurements employed a sonar system (Kongsberg Simrad SM 2000) operating at 200 kHz and mounted on the remotely operated vehicle Jason, operated by the Deep Submergence Group of the Woods Hole Oceanographic Institution. This sonar was used to observe diffuse flow using acoustic scintillation thermography (AST) [*Rona et al.*, 1997; *Johnson et al.*, 2002] and to obtain three-dimensional images of plume backscattering strength from which plume structure can be inferred [*Rona et al.*, 1991; *Bemis et al.*, 2000; *Rona et al.*, 2001].

[4] The Doppler technique reported here employs a standard signal processing method to estimate the component of velocity along the sonar line-of-sight. One of the main technical challenges is to use such single-direction data to infer the vertical component of velocity, and to do this with sufficient accuracy and spatial resolution to allow tests of plume models. The method exploits certain geometric properties of plumes to allow estimation of the vertical component of velocity. Averaging over times of several minutes is required to reduce statistical error to acceptable values.

2. Experimental Setting

[5] A discussion of the experimental situation is useful in order to set the stage for the discussion of plume velocity measurements. The sonar data were acquired with Jason stationary, sitting on the West wall of the Endeavour segment near the Grotto vent complex. Video observations showed that the main Grotto plume is produced by coalescence of at least five vents within a 3 m × 3 m area. The summed areas of these vent orfices was equal to that of a circle having diameter 20 cm, and the initial velocity at each orfice was approximately 100 cm/s as measured by video tracking of eddy structure against a vertical measuring rod. All these visual estimates have uncertainty of about ±20%. The temperature of the vent water was determined to be 359°C using a thermistor probe on Jason. Owing to the turbidity of the water near the summit of Grotto, some vents may have been missed in the video survey. Another potential complication arises from the copious discharge of clear water from the lower flanks of the Grotto edifice. Portions of this water trapped under flanges had temperatures of 300°C and may have influenced plume formation. This is a significant issue, as the sonar data reported here were taken during slack tidal current, when the clear water is less likely to be advected away from the main plume and more likely to mix with it. The several smaller plumes issuing near the summit of Grotto are estimated to have coalesced at a height of about 4–5 m. A significantly lower height of coalescence would have been observable in the video imagery and a significantly greater height would have allowed resolution of separate plumes by the sonar. Owing to sidelobe interference by the Grotto edifice, the sonar could not image plume structure for heights less than 5 m.

[6] Three-dimensional Doppler data were obtained by a combination of time gating (for resolution in range), digital beamforming (for resolution in azimuth), and mechanical scanning (for resolution in elevation). At each sonar elevation setting, an azimuthal interval of 120° was covered by 128 receiving beams, as shown in Figure 1. It should be noted that "sonar elevation" as used in this paper is the angle with respect to the horizontal of the middle two beams of the sonar. If the roll of the platform is zero, the other beams all have smaller elevation angles, with the outermost beams having the smallest elevation. The azimuthal and elevation resolution are both equal to the sonar beamwidth, 1.4° between half-maximum-power points. The Doppler measurements employed a transmitted

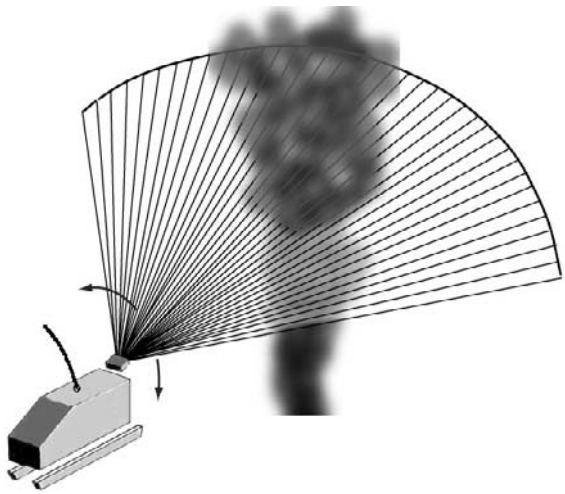

Figure 1. Illustration of the use of multiple sonar receiving beams to provide resolution in azimuth, with the sonar platform (the ROV Jason) stationary on the seafloor, and with mechanical scanning used to provide resolution in elevation.

pulse of rectangular envelope with a length of 1.2 ms. For 3-D Doppler measurements, sonar elevation was changed from approximately horizontal to nearly vertical in 1° steps with a time interval of 4.7 s between steps. At each elevation step, a burst of ten identical 1.2 ms pulses was transmitted with separation of 0.2 s, and a total time of about 6 min was required to complete one vertical sweep of the plume. The sonar employs time-varying gain, which increases the gain as a function of range in order to place all parts of the echo time series within the linear portion of the response of the unit's amplifiers and analog-to-digital converters. The primary factor limiting the range of the measurements reported here was noise originating from Jason rather than non-linearity of the electronics.

[7] Two-dimensional "slices" through the main Grotto plume were obtained by repeated transmissions at a fixed sonar elevation angle of 37°. Bursts of 16 pulses of 1.2 ms length were transmitted at an interval of 3.8 s with a time separation of 0.235 s between pulses. The data set reported here consists of 75 such bursts, with a total data acquisition time slightly less than 5 min.

[8] The sonar system was calibrated to record absolute backscatter pressure. The squared magnitude of backscattered pressure is converted to differential backscatter cross-section per unit volume (units m^{-1}). While the mechanism responsible for scattering has not been identified with certainty, it is very likely due to Rayleigh scattering by individual particles in the plume [*Palmer*, 1996]. This mechanism is not central to the present work, and it is possible that the backscattered signal is due at least in part to temperature fluctuations characteristic of the turbulent plume structure [*Oeschger and Goodman*, 2003] or to random density fluctuations resulting from mass loading by the particulates. Random salinity structure may be less important owing to the relatively small contrast of the vent fluid with ambient water (5 psu), but should not be discounted at this point. Whatever the scattering mechanism, the primary assumption made here, as in most Doppler measurements, is that the scattering structures are passive tracers advected by the flow. This is the case for Rayleigh scattering provided gravitational settling of the particles is negligible and is plausible for scattering by random structure, as the scale of the structure responsible for backscatter (not including particulate Rayleigh scattering) is one-half the acoustic wavelength, or about 3.75 mm. As will be seen, the backscatter cross-section data were used to determine the plume centerline, a first step in compensating for ambient current.

3. Measurement of Vertical Velocity

[9] Doppler shift provides a measurement of the component of velocity along the sonar line of sight, here denoted the "radial component". Geometric corrections can then be applied to determine the vertical component of velocity. Doppler shift can be estimated using conventional "incoherent" processing in which the first moment of the signal spectrum is estimated from the phase of the complex covariance [*Rummler*, 1968; *Pinkel and Smith*, 1992]. Although the processing algorithm employed is not new, some details will be given in the Appendix in order to completely specify the method. As mentioned earlier, the novel aspect of this work is not in signal processing, but in the geometric methods used to determine the spatial dependence of the vertical component of velocity

from single-direction sonar data. As outlined in the Appendix, the covariance was estimated by averaging over a time window of length, T. For all results reported here, this window width was chosen such that the corresponding range interval, ($cT/2$) was 2 m, where c = 1490 m/s is the speed of sound. In order to reduce statistical fluctuation in the covariance estimate, further averaging was performed over the pings within a burst (10 or 16). An expression for the precision of the Doppler shift estimate in terms of the averaging window width and number of pings is given in the Appendix. To differentiate between other sources of error, this error will be denoted intrinsic error, as it is determined by sample size and cannot be reduced by, e.g., filtering or an increase in transmitter power. Another important source of error is noise, of which two different types were evident. Occasional impulsive noise events were simply edited out by omitting all data from the affected burst. These were short pulses originating in the machinery on board JASON, but it is not certain whether they were electronic or acoustic in nature. Tonal noise was present in all data, and was reduced by means of narrow-band notch filtering. As the residual noise is non-random, theoretical estimates of RMS error due to noise are of little value. Error due to residual noise was estimated by applying the Doppler estimation algorithm to portions of the echo that were deemed essentially free of useful signal. This procedure will be illustrated with an example from the Grotto data set. Another major source of error results from turbulent fluctuations in the plume structure. Again, theoretical error estimates are of little value, so sample variance estimates are used to determine the corresponding uncertainties in measured velocity. These variances incorporate fluctuations due to three main causes: plume structure variations, noise, and the intrinsic error discussed above.

[10] To reduce the effect of unwanted echos from the edifice returning through sonar sidelobes, the coherent average of the signals received from each burst is subtracted from each member of the burst. In effect, this removes the zero-Doppler component of the signal, suppressing signal energy coming from the (unmoving) edifice. A similar strategy is employed for plume imaging of the backscatter cross-section, but the residual sidelobe signal is still sufficient to mask the plume at heights below 5 m.

[11] The sonar system provides 3-D spatial resolution, but only resolves one component of velocity, the "radial" component (the component along the sonar line-of-sight). The method used to determine vertical velocity is discussed in the Appendix. In this method, the plume "centerline" is estimated as the locus of maximum (with respect to the horizontal coordinates) backscatter cross-section data taken from an imaging data run contiguous in time with the Doppler data run of interest. A crucial assumption is made at this stage: the centerline is assumed to be a streamline. With this assumption, the Doppler and centerline data suffice to determine all three components of the velocity vector at each point along the centerline. Finally, it is assumed that the horizontal components of the centerline velocity are equal to the ambient current. Thus the measured radial component of velocity can be corrected by subtracting the radial component of the ambient current velocity, and the vertical component of velocity is obtained by dividing by the sine of the elevation angle of the point of interest.

[12] The assumption that flow velocity (after subtraction of ambient current) is vertical introduces error owing to contamination by the horizontal components of plume velocity. Horizontal growth of the plume with height demands an intrinsic horizontal particulate velocity directed away from the centerline. As shown in the Appendix, the error in flux determinations due to neglect of the horizontal velocity component is only about 2%.

[13] After processing to estimate vertical velocity, the data are transformed from the sonar coordinate system to a system aligned with earth coordinates with the sonar at the origin. This transformation uses platform attitude and heading data. After coordinate transformation, the data are resampled onto 2-D or 3-D grids.

4. Three-Dimensional Data

[14] Three-dimensional images showing isosurfaces of vertical velocity for two successive sweeps

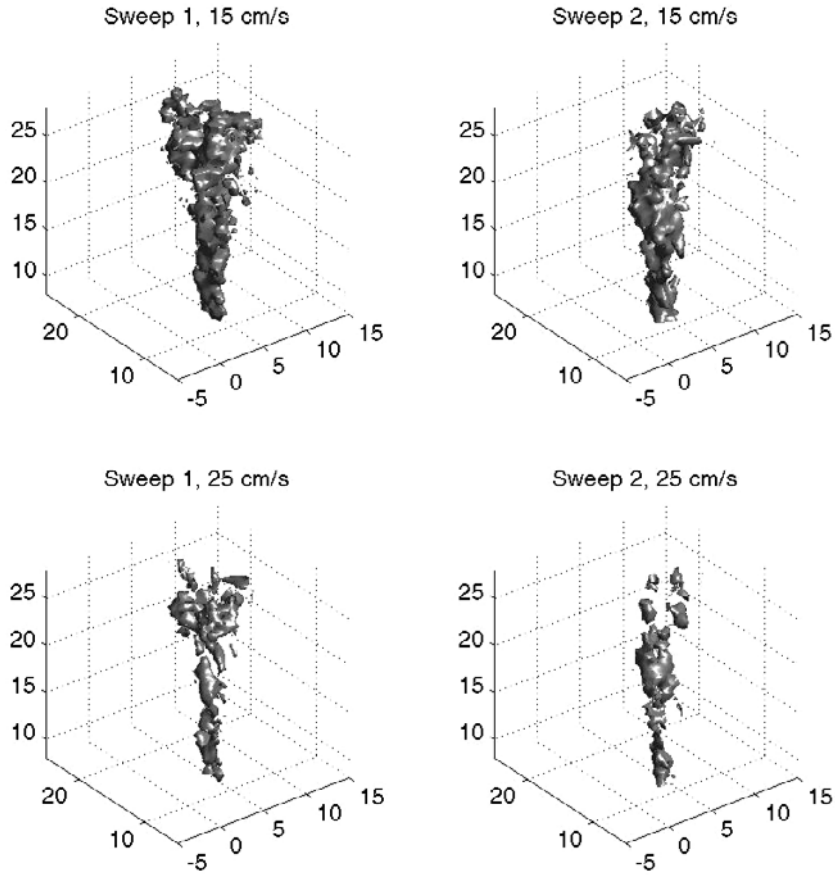

Figure 2. Isosurfaces of vertical velocity for the main Grotto plume. The panels on the left show the velocity structure of the first sweep, and the panels on the right-hand side show the second sweep, approximately 6 min later. The origin of the coordinate system is at the sonar, with x-coordinate increasing from −5 to 15 m toward the east and the y-coordinate increasing from 5 to 25 m toward the north. The vertical scale is the height above the sonar in m. The sonar was at a depth of 2191 m, approximately 2 m below the vent, at UTM coordinates 492618 m E, 5310655 m N. As indicated at the top of each panel, the velocity isosurfaces were evaluated at 15 cm/s and 25 cm/s.

of the main Grotto plume are shown in Figure 2. These data are from measurement run 111, 25 July 2000, 22:34 GMT; subsequent sweeps were lost due to a malfunction. The processed data were placed on a grid with 0.5 m spacing. With only two sweeps available, each sweep was treated as a snapshot, and no averaging was performed. Using the expression given in the Appendix, the intrinsic RMS velocity imprecision is 14 cm/s for the 3-D measurements. This large error is due to the small amount of averaging relative to that used in acoustic Doppler current profilers [*Hansen*, 1986]. This error is comparable in magnitude to the estimated velocities; consequently, the 3-D snapshots can only provide an approximate picture of the plume velocity structure. Given the measurement error and the fact that the plume was nearly vertical during the measurements, the ambient velocity correction procedure outlined in the Appendix was not applied. The first sweep in Figure 2 reveals an event in which a volume of high velocity fluid was transported to rather high elevation in the plume. The next sweep shows velocity isosurfaces without the pronounced bulge at greater elevation. In interpreting these images it must be noted that they are formed by sweeping from one elevation extreme to another (low to high for the first sweep, high to low for the second) with a time of 6 min between the midpoints of the two sweeps. As a consequence, these images are not really instantaneous snapshots. The thresholding that defines the isosurfaces creates the illusion of well-defined

volumes, but it must be remembered that the spatial resolution provided by the sonar is 1.4° in angle and 2 m in range, or about 0.5 m × 0.5 m × 2 m at 20 m range. This causes some spreading of the plume images, but this distortion is small compared to the other measurement errors.

[15] Three-dimensional Doppler data having better statistics than those of the present example would be of great value in testing plume models, allowing comparison of profiles of vertical velocity and volume flux with model predictions. With 16-ping bursts, averaging over 10 sweeps would reduce the intrinsic RMS velocity imprecision to about 3.5 cm/s, an acceptable value. With the rotator system used in VIP 2000, this would require a data gathering period of about 1 hour, raising questions as to stability of the plume over such a long time period. More rapid scanning is possible, in principle.

5. Two-Dimensional Data

[16] In the 2-D measurements, 16 pings were transmitted in short bursts and averaging over a total of 75 bursts reduced the intrinsic RMS velocity imprecision to a value of 1.3 cm/s, sufficiently low to allow quantitative analysis. Figure 3 shows a 2-D "slice" through the plume from run 168 on 27 July 2000, 02:43 GMT. The sonar elevation angle was 37°, and the sonar was at a depth of 2187 m, approximately 2 m below the vent, at UTM coordinates 492611 m E, 5310654 m N. All slices in the figure are projected onto a horizontal plane and gridded with 0.5-m spacing. The upper left panel shows the estimated mean vertical velocity, with the white dashed line indicating the constant-range one-dimensional (1-D) slice to be discussed later. The upper right panel shows the volume scattering strength (the decibel equivalent of backscatter cross-section, that is, the cross-section is operated on with 10 $\log_{10}$) with the white line indicating the plume centerline projected onto a horizontal plane. The lower right panel indicates the RMS error in the mean estimate of the upper left panel due to all causes, including variability of the flow over the measurement period. The lower left panel shows the portion of this error that is due to noise and signal fluctuation (intrinsic error). The noise contribution was estimated by applying the Doppler processing algorithm to a portion of the sonar field of view containing no evident plume return and scaling the resulting variance by the inverse of 75 and the inverse of the signal level (the estimated backscatter cross-section). The sharp edge of the velocity map is due to the windowing discussed below and does not indicate the true spatial resolution. Resolution is roughly 2 m in range (distance from origin) and 0.5 m in the perpendicular direction.

[17] To quantify tipping of the plume due to ambient current, the plume centerline was estimated by fitting a second-order polynomial to the peak backscatter cross-section data taken from a 3-D run made 20 min before run 168. This centerline spans the height range 5–30 m and is shown as the short curve in the upper right panel of Figure 3, white above the slice plane and black below. The centerline passes though the slice plane at a height of 16 m above the vents. The plume has a slight tilt (about 4° at 16 m height) toward NNE due to ambient current. Using the unit vector tangent to the centerline and the measured radial component of velocity, the mean velocity vector on the centerline at a height 16 m above the vents is (0.9, 1.5, 18.7) cm/s (E, N, and upward) with error of about 1 cm/s for the horizontal components and error of about 2 cm/s for the vertical component. The vertical velocities shown in the upper left panel were obtained using the procedure detailed in the Appendix. The velocity data have been windowed to include only the region for which the backscatter cross-section is larger than 4% of its peak (central) value. This is done in order to insure that the signal/noise is sufficiently high for accurate Doppler estimation. The lower right panel of Figure 3 shows the total RMS error computed as the sample standard deviation divided by the square root of 75. This fluctuation includes all sources of random error and falls in the range 1–3 cm/s. It is dominated by fluctuation in the plume velocity structure as can be seen by inspection of the lower left panel of Figure 3. This panel shows that the error due to noise and signal fluctuation (intrinsic error) is small in comparison to the total error. Recall that the intrinsic RMS error due to signal fluctuation is

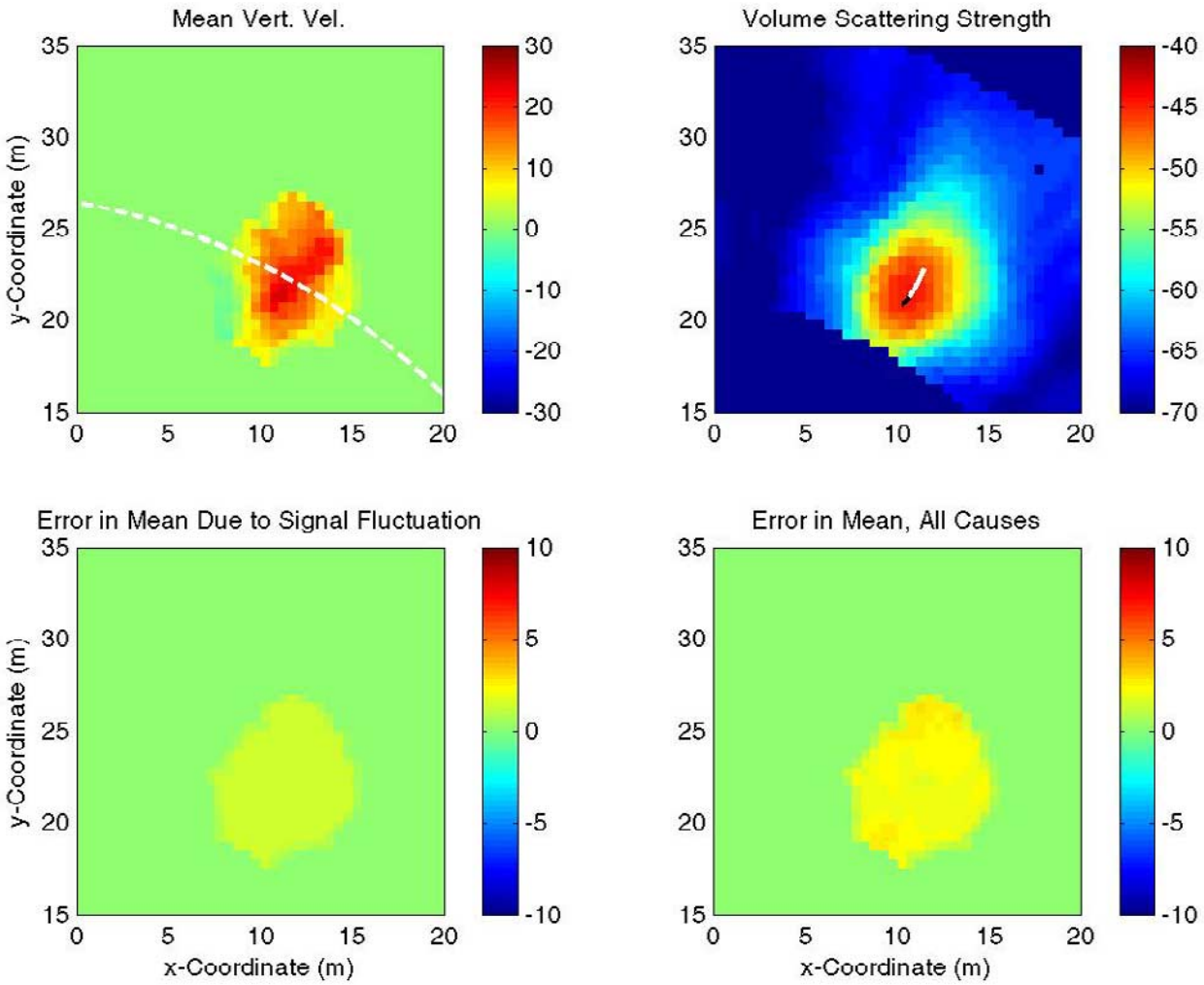

Figure 3. Two-dimensional slices though the Main Grotto plume at a sonar elevation angle of 37°. The upper left panel shows the estimated mean vertical velocity (cm/s, linear scale) with dashed line indicating the constant-range 1-D slice to be displayed in other figures. The upper right panel shows the volume scattering strength (the decibel equivalent of backscatter cross-section). The short white line shows the portion of the plume centerline above the slice plane; the shorter black line the portion below. The lower right panel indicates the RMS error (cm/s) in the mean estimate of the upper left panel, and the lower left panel shows the portion of this error (cm/s) that is due to noise. The x- and y-coordinates are in m (east and north) defined relative to Jason, which occupied a different position than for the data of Figure 2.

1.3 cm/s, and accounts for most of the error depicted in the lower-left panel.

[18] The net volume flux of fluid though the 2-D slice surface can be found by integrating the vertical velocity over the horizontal coordinates. The estimated mean flux is 5.5 m^3/s with an RMS statistical error (computed from the sample variance of the fluxes of each of the 75 bursts) of 0.4 m^3/s. There is a slight upward bias in this flux estimate owing to its computation over an inclined, rather than horizontal plane. Owing to entrainment, volume flux increases with height at a rate faster than the first power of height. Thus the excess flux over the higher portion of the plane is not fully compensated by the reduced flux over the lower portion. Computations using the present geometry and the model of *Morton et al.* [1956] as modified by *Speer and Rona* [1989] show that this bias in the flux estimate should only be about 1%. A more significant issue is the possible mixing of the smoker plume with the clear, hot water emanating

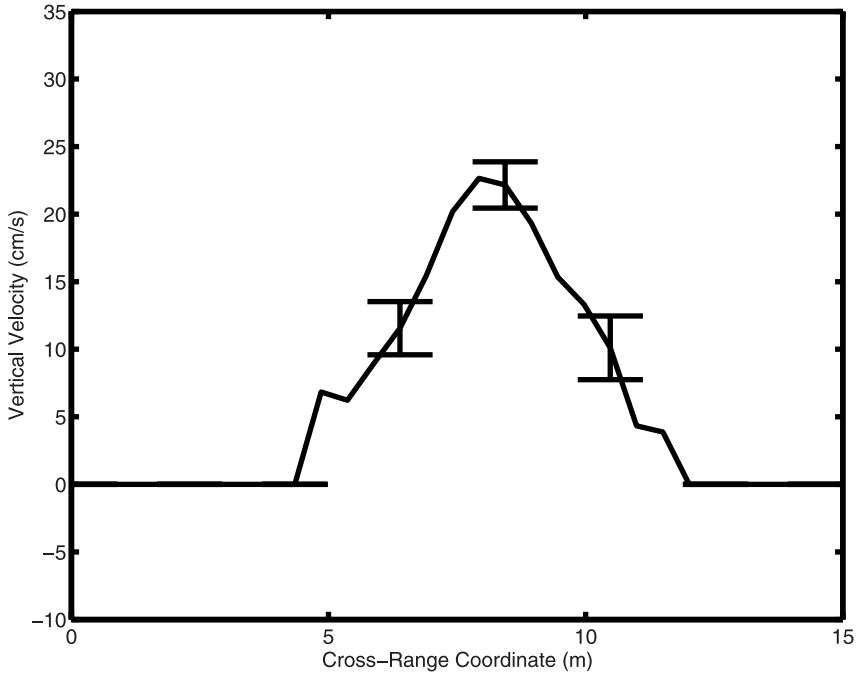

Figure 4. Mean velocity field along the 1-D slice indicated in Figure 4. Representative errors bars are shown for a few data points.

from the flanks of the edifice. As noted earlier, it is possible that this contributes significantly to the measured flux and may complicate comparisons with models. Dividing the measured volume flux by the initial flux computed from initial velocity and equivalent orfice diameter, the flux has increased by a factor 175 at a height of 16 m. This entrainment ratio is consistent with preliminary calculations using the model mentioned above, but is substantially smaller than the ratios reported for a plume on the North Cleft Segment of the Juan de Fuca Ridge [*Feely et al.*, 1994], which were of the order of 1000 at heights similar to that of the present case.

[19] The dashed circular arc in the upper left panel of Figure 3 indicates the locus of data chosen for one-dimensional plots of the velocity field. These data were extracted from a single range bin of the ungridded data. Figure 4 shows the mean velocity with error bars corresponding to the total error depicted in the lower right panel of Figure 3. The zero values of velocity are not actual estimates, they merely define the region for which error was deemed too large for analysis. This is the region defined by the 2-D window discussed earlier. This velocity profile is consistent with the Gaussian shape observed in laboratory measurements [*Papanicolaou and List*, 1988], but the errors are too large to permit a definite comparison. The measured diameter/height ratio (0.2) at 16 m height is consistent with values obtained by the Flow Mow group [*Stahr et al.*, 2002] for the main Grotto plume at a height of 40 m. The broadening due to sonar resolution can be estimated as approximately 0.04 m by adding the true width and the resolution in quadrature.

6. Discussion

[20] The primary measurement issue addressed in this work is whether a sonar without multiple intersecting beams (as needed to measure the velocity vector at a point in space) can measure the vertical velocity structure of a high-temperature hydrothermal plume. This has been shown to be possible by taking advantage of the particular structure of hydrothermal plumes. A method has been demonstrated for correcting bias due to ambient current using concurrent sonar backscatter strength images to determine the tilt of the plume centerline, in effect using the plume itself to

measure ambient current. The actual cause of backscattering has not been determined, and may be either due to Rayleigh scattering by particulates, or to turbulent fluctuations on millimeter scales in temperature, salinity or particle concentration.

[21] The Doppler measurements reported here used a multibeam imaging sonar to obtain 2-D and 3-D measurements of plume flow velocity fields that cannot be achieved by conventional means. The 3-D measurements show temporal variability in the gross plume structure on time-scales of minutes. The 2-D data provide a volume flux of 5.5 m^3/s at a height of 16 m. Comparison with models such as that of *Morton et al.* [1956] will have to confront uncertainties arising from multiple sources, including nearby diffuse flow.

[22] The primary source of error in the 2-D measurements was the inherent fluctuation in plume structure, but was sufficiently small (about 3 cm/s) to permit quantitative analysis. The error in the 3-D data reported here was larger than that of the 2-D measurements and was primarily due to small sample size. This error can be reduced to acceptable values in future measurements by lengthening observation times to about 1 hour or by using more rapid scanning of the plume than was possible in the VIP 2000 experiment. Such measurements would permit estimation of vertical profiles of velocity and transport and should be particularly useful in testing plume models and calculating fluxes [*Morton et al.*, 1956; *Turner*, 1986; *Speer and Rona*, 1989; *McDuff*, 1995]. The integrated product of vertical velocity and backscatter cross-section is proportional to particulate flux if the Rayleigh scattering mechanism is dominant. If the suspended particles are a conservative tracer, this flux would be independent of height. Settling of larger particles would be noted as a diminution of this flux with height.

Appendix

[23] This appendix give details of the Doppler estimation algorithm, the precision of this estimate, and the assumptions and calculations used to deduce the vertical component of velocity from the measured radial component.

[24] The Doppler shift in radians/s, ω_D, is given by the following estimator, where "arg[A]" denotes the phase angle in radians of the complex number A.

$$\omega_D = \frac{1}{\Delta t}\arg\left[\sum_{b=1}^{N_b}\sum_{p=1}^{N_p}\int_{t-T/2}^{t+T/2} S_{bp}(t')S_{bp}^{*}(t'+\Delta t)dt'\right] \quad \text{(A1)}$$

In practice, the time integral is replaced by a sum over time domain samples, but the sampling rate for the data presented here was sufficiently high (32 kHz) that the sum approximates the integral accurately. In the usual fashion, the radial component of velocity, V_r, is found from the Doppler shift as follows:

$$V_r = \frac{c\omega_D}{2\omega_0}, \quad \text{(A2)}$$

where ω_0 is the center frequency of the sonar expressed in rad/s. In (A1), $S_{bp}(t)$ is the demodulated (baseband) signal whose phase angle and magnitude are equal to the time-varying phase and amplitude of the received time domain signal, such that the true signal is the real part of $S_{bp}(t)$ $\exp(-i\omega_0 t)$. The sampling interval is denoted Δt, the index p denotes the ping number within a "burst" consisting of N_p pings, and b denotes the "burst" number, with the total number of bursts being N_b. For the 3-D data reported here, $N_p = 10$, $N_b = 1$ and, for the 2-D data $N_p = 16$, $N_b = 75$. The range to the center of the volume at which Doppler shift is estimated is (ct/2).

[25] An expression for the precision of the Doppler shift estimate can be derived by assuming the sonar signal is a complex Gaussian random process and then computing the second moment of the covariance estimate (A1). This involves a fourth moment of the signal. The result is

$$\sigma_\omega^2 = \frac{2/\tau - 1/(2T)}{N_b N_p T}. \quad \text{(A3)}$$

This expression can be obtained from the more general analysis of *Miller and Rochwarger* [1972] after significant manipulation of their equation (30). The angular frequency variance, σ_ω^2, is in units rad^2/s^2, τ is the pulse length (1.2 ms), T is the averaging window width (2.7 ms), and the product $N_b N_p$ is the number of independent measurements

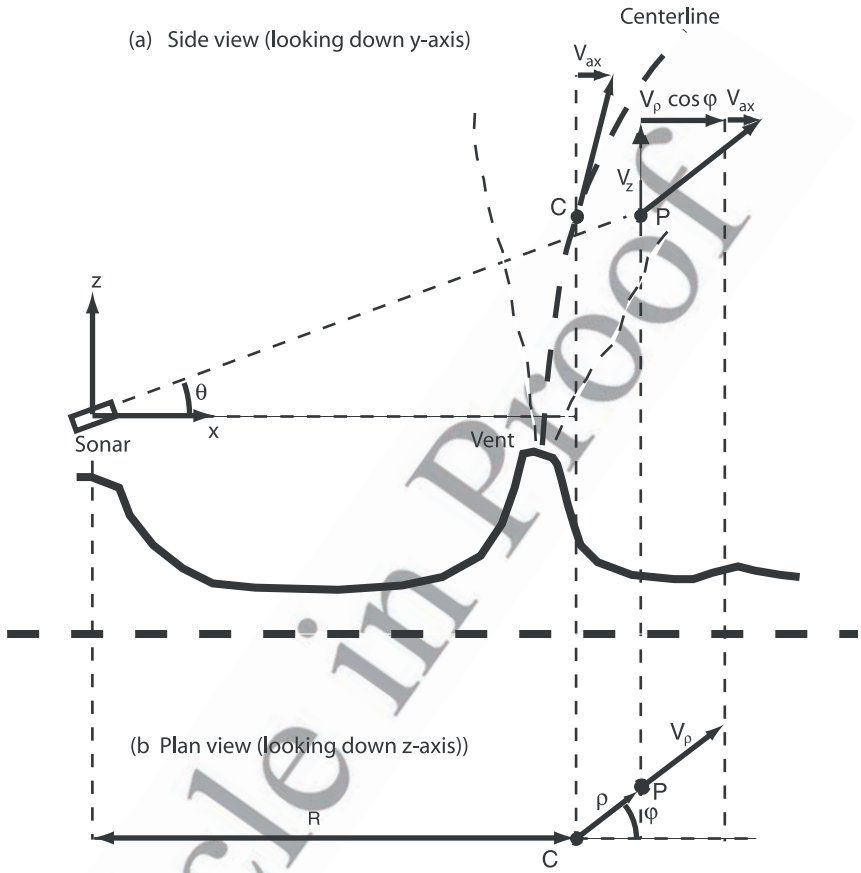

Figure A1. Schematic illustration of (a) method of determining ambient velocity, $\boldsymbol{V}_a$, assumed to be the same at points C and P, and (b) coordinate system used to obtain equation (7) for the contamination of the estimated vertical velocity, V_z, by the intrinsic horizontal component of velocity, V_ρ, responsible for spreading of the plume. In Figure A1a, the plume centerline is denoted by the heavy, curved dashed line, and the approximate plume boundaries are denoted by lighter, wavy dashed lines.

used in forming the estimate. The error represented by σ_ω^2 will be denoted intrinsic error. Finally, the imprecision in velocity estimates due to intrinsic error is

$$\Delta V = \frac{c\sigma_\omega}{2\omega_0}. \tag{A4}$$

The method used to determine the vertical component velocity given the radial component is illustrated in Figure A1, in which the coordinate system is centered on the sonar with *x axis* in the plane of the line of sight. The point "P" in the figure represents an arbitrary point in the plume. As a first step in determining vertical velocity, ambient horizontal current is estimated from bending of the plume at the point "C" at the same height as P. First, the plume "centerline", indicated by a heavy, curved, dashed line in Figure A1a, is estimated from 3-D backscatter cross-section data. Using 3-D gridded backscatter cross-section data, the horizontal (x and y) coordinates corresponding to the maximum backscatter cross-section at each value of the vertical (z) coordinate are determined. Second-order polynomials are fitted to $x(z)$ and $y(z)$ to define the centerline. The term "centerline" is a misnomer in cases of strong ambient current, as the plume may depart substantially from axisymmetry. Next, the radial component of velocity is also evaluated at C on the centerline, and the velocity vector on the centerline is assumed tangent to the centerline. The Doppler and centerline data are then used to determine all three components of the velocity vector at C according to the equation

$$\boldsymbol{V}_c = \frac{V_{rc}}{\hat{\boldsymbol{e}}_c \cdot \hat{\boldsymbol{e}}_{rc}} \hat{\boldsymbol{e}}_c. \tag{A5}$$

In (A5), $\boldsymbol{V_c}$ is the velocity vector at C, a function of height, z, V_{rc} is the measured radial velocity at height, z, on the centerline, $\hat{\boldsymbol{e}}_c$ is a unit vector tangent to the centerline, and $\hat{\boldsymbol{e}}_{rc}$ is a unit vector pointing from the sonar to the centerline at C. It should be noted that the ambient current correction does not require detailed information on the development of plume tilt over lower heights. Finally, it is assumed that the horizontal components of the centerline velocity are equal to the ambient current, that is, with reference to Figure A1, $V_{ax} = \boldsymbol{V}_{r0} \cdot \hat{\boldsymbol{x}}$, $V_{ay} = \boldsymbol{V}_{r0} \cdot \hat{\boldsymbol{y}}$ where $\hat{\boldsymbol{x}}$ and $\hat{\boldsymbol{y}}$ are the usual Cartesian unit vectors. Thus the measured radial component of velocity is corrected by subtracting the radial component of the ambient current velocity, and the vertical component of velocity is obtained by dividing by the sine of the elevation angle of the point, P, in question:

$$V_z = \frac{V_r - V_{rc}[(\hat{\boldsymbol{e}}_{c0} \cdot \hat{\boldsymbol{x}})(\hat{\boldsymbol{e}}_r \cdot \hat{\boldsymbol{x}}) + (\hat{\boldsymbol{e}}_{c0} \cdot \hat{\boldsymbol{y}})(\hat{\boldsymbol{e}}_r \cdot \hat{\boldsymbol{x}})]}{\sin\theta}, \qquad \text{(A6)}$$

where $\sin\theta = \hat{\boldsymbol{e}}_r \cdot \hat{\boldsymbol{z}}$. Here, quantities that do not bear the subscript c are defined for any arbitrary point, P, over the entire observation volume, while those having this subscript are to be evaluated on the centerline at the z-coordinate of interest, but are independent of x and y. The unit vector $\hat{\boldsymbol{e}}_r$ points from the sonar to each observation point. It should be remembered that, while the ambient current is assumed to be constant with respect to the horizontal coordinates (x, y), it is *not* assumed to be constant with respect to height, z.

[26] Horizontal growth of the plume with height demands an intrinsic horizontal particulate velocity directed away from the centerline. The velocity is assumed to vanish on the centerline, but must increase with radial distance to a value whose ratio with respect to the vertical component may be roughly estimated as equal to the radius/height ratio, a/z, of the plume. Using a new coordinate system, defined in Figure A1b, geometric considerations can be used to show that the numerator of (A6) (the corrected radial velocity component) is

$$V_l = \sin\theta\left[V_z + \frac{\rho + R\cos\varphi}{z} V_\rho\right], \qquad \text{(A7)}$$

where R is the horizontal distance between the sonar and plume centerline at point C, and θ is the elevation angle of the line of sight between the sonar and the measurement point, P. This point has cylindrical coordinates (ρ, φ, z) with respect to the centerline, with z being the height of P above the sonar (not the vent orfice). In this coordinate system, V_z and V_ρ are the vertical and horizontal (outward) components of velocity. The factor $\sin\theta$ is removed by the correction defined in (A6), leaving the term containing V_ρ as a contaminant. This term has two parts: the first part is proportional to the radius/height ratio ρ/z, a small number, and the second part is proportional to the range/height ratio, R/z, a number of order unity in the measurements to be discussed. As noted above, the horizontal velocity is smaller than the vertical velocity by a factor of approximately a/z, where a is the plume radius at the height in question. Here it has been assumed that the sonar is approximately at the same depth as the vent, as in these measurements. It follows that the fractional errors corresponding to the two terms are of order $(a/z)^2$ and a/z. From the results to be given, a/z is about 0.13, so the fractional errors represented by the first and second terms are roughly 0.017 and 0.13, respectively. The larger error term does not contribute to flux determinations, which involve integrating over horizontal coordinates, hence averaging over azimuthal angle. Thus the error in flux determinations due the geometric factors treated here is only about 2%, and will be a positive bias in this amount.

Acknowledgments

[27] We acknowledge outstanding support of our acoustic imaging cruises received from the Deep Submergence Group and the ROV Jason team of the Woods Hole Oceanographic Institution and the marine office, officers and crew of the R/V T.G. Thomson of the University of Washington. This research was supported by NSF RIDGE Program Grant OCE 98-18841. A portion of C. Jones' work was supported under OCE 99-11523.

References

Baker, E. T., C. R. German, and H. Elderfield, Hydrothermal plumes over spreading-center axes: Global distributions and geological inferences, in *Seafloor Hydrothermal Systems: Physical, Chemical, Biological, and Geological Interactions*, *Geophys. Monogr. Ser.*, vol. 91, edited by S. Humphris et al., pp. 47–71, AGU, Washington, D.C., 1995.

Bemis, K. G., P. A. Rona, D. R. Jackson, C. D. Jones, D. Palmer, D. Silver, and R. Gudlavalletti, Multi-scale time-dependent behavior of hydrothermal plumes at Grotto Vent, Main Endeavour Vent Field, Endeavour segment, Juan de Fuca Ridge: A time series of acoustic images (abstract), *Eos Trans AGU.*, *81*(46), Fall Meet. Suppl., F629, 2000.

Feely, R. A., G. J. Massoth, J. H. Trefry, E. T. Baker, A. J. Paulson, and G. T. Lebon, Composition and sedimentation of hydrothermal plume particles from north cleft segment, Juan de Fuca Ridge, *J. Geophys. Res.*, *99*, 4985–5006, 1994.

Hansen, D. S., Oceanic incoherent Doppler sonar spectral analysis by conventional and finite-parameter modeling methods, *IEEE J. Oceanic Eng.*, *11*, 26–41, 1986.

Johnson, H. P., et al., Survey studies hydrothermal circulation on the northern Juan de Fuca Ridge (abstract), *Eos Trans. AGU*, *83*, 73, 2002.

Lupton, J. E., Hydrothermal plumes: Near and far field, Seafloor Hydrothermal Systems, in *Seafloor Hydrothermal Systems: Physical, Chemical, Biological, and Geological Interactions*, *Geophys. Monogr. Ser.*, vol. 91, edited by S. E. Humphris et al., pp. 317–346, AGU, Washington, D.C., 1995.

McDuff, R. E., Physical dynamics of deep-sea hydrothermal plumes, Seafloor Hydrothermal Systems, in *Seafloor Hydrothermal Systems: Physical, Chemical, Biological, and Geological Interactions*, *Geophys. Monogr. Ser.*, vol. 91, edited by S. E. Humphris et al., pp. 357–368, AGU, Washington, D.C., 1995.

Miller, S. M., and M. M. Rochwarger, A covariance approach to spectral moment estimation, *IEEE Trans. Info. Th.*, *18*, 588–596, 1972.

Mitsuzawa, K., The application of ADCP to the measurement of current system at the hydrothermal active areas, paper presented at the *IEEE/OES Seventh Working Conference on Current Measurement Technology*, 246–249, Int. Elec. Elec. Eng., New York, 2003.

Morton, B. R., G. I. Taylor, and J. S Turner, Turbulent gravitational convection from maintained and instantaneous sources, *Proc. R. Soc. London Ser. A*, *234*, 1–23, 1956.

Oeschger, J., and L. Goodman, Acoustic scattering from a thermally driven buoyant plume revisited, *J. Acoust. Soc. Am.*, *113*, 1353–1367, 2003.

Palmer, D. R., Rayleigh scattering from nonspherical particles, *J. Acoust. Soc. Am.*, *99*, 1901–1912, 1996.

Palmer, D. R., and P. A. Rona, Comment by R. E. Thomson et al. on "Acoustic Doppler current profiler observations of a mid-ocean ridge hydrothermal plume", *J. Geophys. Res.*, *95*, 5409–5412, 1990.

Papanicolaou, P. N., and E. J. List, Investigations of round vertical turbulent buoyant jets, *J. Fluid Mech.*, *195*, 341–391, 1988.

Pinkel, R., and J. A. Smith, Repeat-sequence coding for improved precision of Doppler sonar and sodar, *J. Atmos. Oceanic Technol.*, *9*, 149–163, 1992.

Rona, P. A., D. R. Palmer, C. Jones, D. A. Chayes, M. Czarnecki, E. W. Carey, and J. C. Guerrero, Acoustic imaging of hydrothermal plumes, East Pacific Rise, 21°N, 109°W, *Geophys. Res. Lett.*, *18*, 2233–2236, 1991.

Rona, P. A., D. R. Jackson, T. Wen, C. Jones, K. Mitsuzawa, K. G. Bemis, and J. G. Dworski, Acoustic mapping of diffuse flow at a seafloor hydrothermal site: Monolith Vent, Juan de Fuca Ridge, *Geophys. Res. Lett.*, *24*, 2351–2354, 1997.

Rona, P. A., K. G. Bemis, D. R. Jackson, C. D. Jones, K. Mizuzawa, D. Palmer, and D. Silver, Acoustic imaging time series of plume behaviour at Grotto Vent, Endeavour Observatory, Juan de Fuca Ridge, *Eos Trans. AGU*, *82*(46), Fall Meet. Suppl., Abstract OS21B-0445, 2001.

Rummler, W. D., Introduction of a new estimator for velocity spectral parameters, *Tech. Memo MM-68-4141-5*, Bell Telephone Lab., Murray Hill, N.J., 1968.

Speer, K. G., and P. A. Rona, A model of an Atlantic and Pacific hydrothermal plume, *J. Geophys. Res.*, *97*, 6213–6220, 1989.

Stahr, F. R., R. E. McDuff, D. R. Yoerger, A. M. Bradley, and K. Nakamura, Heat flux measurements at the Main Endeavour vent field, Juan de Fuca Ridge, *Eos Trans. AGU*, *81*(46), Fall Meet. Suppl., OS52I-03, 2002.

Thomson, R. E., R. L. Gordon, and J. Dymond, Acoustic Doppler current profiler observations of a mid-ocean ridge hydrothermal plume, *J. Geophys. Res.*, *94*, 4709–4720, 1989.

Turner, J. S., Turbulent entrainment: The development of the entrainment assumption and its application to geophysical flows, *J. Fluid Mech.*, *173*, 431–471, 1986.